

A better understanding of the properties of alginate solutions and gels by quantitative magnetic resonance imaging (MRI)

Anna Degrassi ^a, Renato Toffanin ^b, Sergio Paoletti ^{b,c},
Laurance D. Hall ^{a,*}

^a *Herchel Smith Laboratory for Medicinal Chemistry, Cambridge University School of Clinical Medicine, University Forvie Site, Robinson Way, Cambridge CB2 2PZ, UK*

^b *POLY-biós Research Centre, AREA Science Park, Padriciano 99, I-34012 Trieste, Italy*

^c *Department of Biochemistry, Biophysics and Macromolecular Chemistry, University of Trieste, via L. Giorgieri 1, I-34127 Trieste, Italy*

Received 12 June 1997; accepted 11 October 1997

Abstract

A new, fully automated magnetic resonance imaging (MRI) procedure has been used to measure for the first time all the MRI parameters of water in both sodium alginate solutions and calcium alginate gels at concentrations of 1%, 2%, 3%, 4% (w/w). Spin–spin (T_2) and spin–lattice (T_1) relaxation times, magnetisation transfer processes (MT) and diffusion coefficients (D) were measured to evaluate their potential use for studying gelling mechanisms and for determining gel characteristics. Four alginate samples, with different extents of *O*-acetylation were also studied and the use of MRI to discriminate between them was evaluated. © 1998 Elsevier Science Ltd. All rights reserved.

Keywords: Alginate; Gels; MRI

1. Introduction

Because of a total lack of toxicity and an ability to form viscous solutions and gels, alginate is becoming more widespread used in the food industry as a thickening agent, in biotechnology as an immobilisation matrix for enzymes and living cells [1–4] and in medicine and agriculture for controlled release of drugs and pesticides. Gelation of alginates with calcium ions is understood in molecular terms [5]; a

correlation between gel strength and alginate concentration has been established, and relevant properties of calcium alginate gels such as mechanical rigidity, volume stability, swelling and shrinking characteristics have been studied by a variety of techniques [6–8]. Much work has also been done in order to understand how differences in chemical structure influence the functional properties [9,10], which are important to the choice of which type of alginate and gelling methodology are most suitable for each specific application. In particular, it has been observed that an increase in *O*-acetyl content results in a decrease in gel strength [9]. Magnetic resonance

* Corresponding author.

imaging (MRI) has already been successfully used to map the spatial variation of alginate concentration and distribution of pore size in inhomogeneous calcium alginate gels [11], and to track the reaction front during the gelation of sodium alginate by calcium ions [12].

In this paper, we report for the first time the measurement of all the MRI parameters for water in sodium alginate solutions and calcium alginate gels; the aim was to obtain better understanding of the relevant characteristics of alginate samples, such as gel strength, porosity and diffusion properties. Thus, we have considered how MRI can be used to discriminate between different structures and thereby provide better insight to the correlation between chemical structure and physical properties of the gels.

The sequence of studies was as follows. First, it was necessary to decide how best to apply to both alginate solutions and gels the newly developed, fully automated MRI quantitation protocol for measurement of the spin–lattice relaxation time (T_1 -value), the spin–spin relaxation time (T_2 -value), the magnetisation transfer rate (K), the M_{sat}/M_0 ratio, and the diffusion coefficient (D). Second, it was appropriate to establish which of those parameters was most sensitive to the composition of the solutions and gels. Both of those aspects of the work were explored using an alginate which was available commercially in large quantities. The sensitivity of those MRI parameters to variations of gel strength was then evaluated using four alginate samples which had the same composition in terms of guluronic/mannuronic acid ratio but which differed in *O*-acetyl content.

Before discussing the specific results, it is important to place the present MRI study into the more general context of nuclear magnetic resonance (NMR) spectroscopic measurements of the bulk properties of homogeneous polysaccharide solutions. For both solutions or gels of polysaccharides at low concentration, the NMR response will be dominated by the water protons signal. There are two possible pools of water, the ‘bulk water’ pool in which the molecules are tumbling freely, and that corresponding to those molecules which are ‘chemisorbed’ to the surface of the polysaccharide and hence have a far slower tumbling rate. Generally, there will be a rapid exchange of water molecules between those two pools and hence the measured MRI parameters will reflect the concentration-weighted mean of the values for those two pools. Systematic differences between these MR parameters are expected on the basis of the well known influence of molecular motion; thus, in gen-

eral, protons which are less mobile will tend to have shorter relaxation times (T_1 and T_2 values).

The measured magnetisation transfer parameters ($T_{1\text{sat}}$ and M_{sat}/M_0) along with the resulting calculated value of the magnetisation transfer rate (K) also provide information about the mobility of the polymer chain, but by a somewhat more complex mechanism. These magnetisation transfer parameters also depend on the interchange of water molecules which are chemisorbed to the polymer surface with those in the bulk pool, but are dominated by the interchange of protons between ‘bulk’ water molecules and any chemically labile protons on the polysaccharide (hydroxyl and carboxylate in the case of alginate). Any factor which decreases the overall tumbling rate of the polymer will increase the efficiency of the MT processes and thereby will increase K and decrease M_{sat}/M_0 .

There are several further points which are relevant to the present study. The first reflects the fact that while measurements of NMR parameters for bulk solutions are straightforward, equivalent MRI measurements are not only more time-consuming but intrinsically more complex. This is because the long timing of some of the radio frequency pulses used in an MRI protocol inevitably ‘loses’ some of the magnetisation of interest, especially that of molecules which have short T_2 -values. Furthermore, the magnetic field gradients which are required to induce spatial discrimination also influence the MRI responses of any water molecules that are freely diffusing, resulting in a further loss of MRI-detectable protons. Consequently, it is extremely hard to measure accurately by MRI the NMR parameters of water, whereas it is relatively easy for bulk samples to measure all the NMR parameters. Furthermore, the time required for encoding the spatial dimensions of the MR-image means that the necessary MRI scans can take a long time, often tens of hours.

Since in the present study, we are more concerned with changes in the relative values of those MRI parameters than with the absolute values, we have chosen to use an MRI protocol which sacrifices some degree of numerical accuracy in favour of the spatial information available; it also has a further advantage of providing fully automated data-acquisition and data-processing for more than one sample imaged simultaneously. Finally, there is the implicit assumption that decreased mobility of the alginate molecules corresponds to, or implies, increased gel strength. A correlation between gel strength and alginate concentration has already been established and a higher

alginate concentration in gels corresponds to a situation of decreased mobility for alginate molecules which are more restricted and less free to tumble.

2. Results and discussion

For sodium alginate solutions obtained dissolving commercial sodium alginate in 0.2 M NaCl, the key data are the MR parameter of water obtained by bulk measurements; these are summarised in Table 1. Those data show the sensitivity of each of the parameters to concentration variations in the range 1–4%. As summarised in the bottom row, it is clear that the T_2 - and K -values are the most sensitive in this concentration range. When those same parameters were determined using the MRI protocol a significant systematic decrease is observed in the measurement of T_2 which is about 25% lower than the equivalent value from ‘bulk’ T_2 measurement. It is well known that dephasing of transverse magnetisation is enhanced by the diffusion of water molecules through the magnetic field gradients used in an MRI protocol. In addition, T_2 relaxation is enhanced with an increase of the echo time ($T_E = 20$ ms in the MRI protocol; $T_E = 8$ ms in the ‘bulk’ measurement). The T_1 values were systematically lower by ca. 14%. Two different methods for T_1 measurement were used for ‘bulk’ and MRI protocols: the inversion–recovery method is traditionally preferred for ‘bulk’ measurements since it has twice the dynamic range of the saturation–recovery method used for MRI. In contrast, the saturation–recovery technique is generally used in MRI because it is less time-consuming. Systematic errors are known to be associated with the length of time before data are sampled. Thus, in this study, MRI data were collected after a long echo time ($T_E = 20$ ms), whereas for ‘bulk’ measurement some of the early points of the relaxation curve were sampled to obtain a T_1 relaxation curve. The T_{1sat}

values for the MRI protocol were found to be lower by ca. 10%, M_{sat}/M_0 lower by ca. 10% and the K -values increased by ca. 75%. In spite of these differences in the values between ‘bulk’ and MRI measurements, the same internal ratios for 1–4% were found, as indicated in the bottom rows of Table 1, which clearly confirms that although the absolute MRI values are offset systematically compared to the bulk values, the data from the MRI protocol have the same sensitivity to concentration.

It is well known that alginate gels made by dialysis against solutions of calcium ions, are not homogeneous with respect to the distribution of polymer concentration: a higher concentration of alginate forms an interface region in contact with the calcium ion reservoir, and the alginate concentration gradually decreases towards the centre of the gel. It has been demonstrated that gels which are more homogeneous are formed if sodium ions (antigelling ions) are present on both sides of the dialysis membrane used to form the gel [13]. We have followed that synthesis method, but even so an MRI protocol for T_2 -mapping clearly demonstrates that the gels were not homogeneous; for higher concentrations [2%, 3%, 4% (w/w)] a less concentrated zone in the middle of the gels was quite evident in the images (Fig. 1). We compared those results with images obtained for gels formed without the addition of sodium ions, and verified the higher homogeneity of gels formed in the presence of NaCl. In the absence of sodium ions, the band in the middle of the gel was found to be much wider and much less concentrated, and the edges of the gel which first come in contact with calcium ions have a higher alginate concentration when compared to the gels in which antigelling ions had been added. Thus, for gels made in the presence of sodium ions, the increase in T_2 -value for water in the central less concentrated zone compared with that on the edge was about 10%, 20% and 30%, respectively, for 2%, 3% and 4% (w/w) gel concentrations; in contrast,

Table 1

NMR parameters: ‘BULK’ measurements for alginate solutions at different concentrations (% w/w); alginate solutions have been obtained dissolving commercial sodium alginate in 0.2 M NaCl

| Conc. | T_2 (s) | T_1 (s) | T_{1sat} (s) | M_{sat}/M_0 | K (L/s) |
|-------------------|----------------------------|-------------|----------------|---------------|--------------|
| 1% | 1.14 (0.0009) ^a | 2.44 (0.05) | 2.36 (0.02) | 0.91 (0.03) | 0.039 (0.01) |
| 2% | 0.65 (0.0006) | 2.33 (0.06) | 2.05 (0.02) | 0.88 (0.02) | 0.057 (0.01) |
| 3% | 0.41 (0.0002) | 2.10 (0.04) | 1.85 (0.01) | 0.88 (0.02) | 0.060 (0.01) |
| 4% | 0.29 (0.0002) | 1.90 (0.03) | 1.69 (0.01) | 0.87 (0.02) | 0.077 (0.01) |
| Ratio 1:4% (BULK) | 3.93 | 1.28 | 1.40 | 1.04 | 0.51 |
| Ratio 1:4% (MRI) | 3.98 | 1.29 | 1.48 | 1.14 | 0.47 |

^aThe values in brackets represent the error in the fit of the curve to the experimental data.

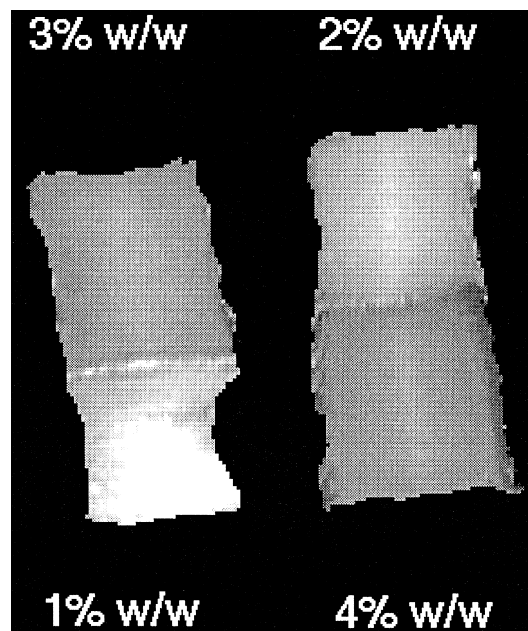


Fig. 1. T_2 -map for alginate gels at different concentrations (% w/w): a less concentrated zone in the middle of the gels is evident for higher concentrations [2%, 3%, 4% (w/w)]. Gels have been obtained dialysing commercial sodium alginate solutions against 0.06 M CaCl_2 containing 0.2 M NaCl.

for gels made without sodium ions, the T_2 enhancements were in the range 100–140%.

These results support the hypothesis [13] that in the absence of sodium ions the gelling mechanism involves an irreversible binding of calcium ions to those alginate chains which first come into contact with the dialysis solution; when sodium ions are present, there is competitive binding of calcium and sodium ions to uronic acid residues, thereby leading to a slower overall of gelation and to more homogeneous gels. Increase in alginate concentration leads to an increase in gel inhomogeneity, as demonstrated by the significant increase in the T_2 -value of water in the middle of the gels made from higher alginate concen-

trations; the relatively slow rate of diffusion of alginate molecules compared with that of the gelling ions means that it is most likely the rate determining step in the gelling process.

Tables 1 and 2 present the data obtained respectively for commercial sodium alginate solutions in 0.2 M NaCl and for calcium alginate gels at different concentrations [1%, 2%, 3%, 4% (w/w)]. For the solutions, the T_2 , T_1 and $T_{1\text{sat}}$ relaxation times decreased (3.9, 1.3, and 1.4-fold) with increased concentration, while there was an increase (2-fold) in the value of MT-rate (K). T_2 seems to be the most interesting parameter, very sensitive to the increased viscosity which is correlated to higher alginate concentrations. K varied linearly with polymer content, but its value was still very low even for very viscous solutions [14]: this demonstrates that the magnetisation transfer process is not very efficient for alginate molecules in solution because the motion of the molecules is still relatively fast.

Because of the unavoidable inhomogeneity of the gels, we chose to average the MRI parameter values for the gel, leaving out the less concentrated band in the middle, which is quite well delineated because of the sharp gradient of T_2 -values at the edges of it. Unfortunately, this implies that the 'real' gel polymer content, to which we wish to attribute the MRI parameter values, will be slightly different from the 'nominal one'. The sole justification is that in such a way the results better represent the dependence of NMR parameters on gel concentration: alginate concentration at the edges of the gel is closer to the 'nominal' one and more indicative of the differences in gel concentration (1%, 2%, 3%, 4%) we were willing to look at.

Table 2 shows for each gel concentration the mean value of three separate measurements, with the value in bracket representing the mean of standard deviation across the region imaged: we chose to represent

Table 2

NMR parameters: MRI measurements for alginate gels at different concentrations (% w/w); alginate gels have been obtained dialysing commercial sodium alginate solutions against 0.06 M CaCl_2 containing 0.2 M NaCl

| Conc. | T_2 (ms) | T_1 (s) | $T_{1\text{sat}}$ (s) | M_{sat}/M_0 | K (L/s) | D (m^2/s) |
|------------|-----------------------------------|-------------|-----------------------|----------------------|-------------|-------------------------------|
| 1% | 123 ^a (7) ^b | 2.31 (0.10) | 1.05 (0.01) | 0.49 (0.02) | 0.50 (0.05) | 2.10×10^{-9} (0.01) |
| 2% | 82 (5) | 2.05 (0.08) | 1.01 (0.07) | 0.43 (0.01) | 0.57 (0.04) | 2.09×10^{-9} (0.01) |
| 3% | 64 (3) | 1.83 (0.08) | 0.87 (0.05) | 0.38 (0.01) | 0.68 (0.04) | 2.09×10^{-9} (0.01) |
| 4% | 48 (3) | 1.63 (0.07) | 0.77 (0.05) | 0.35 (0.01) | 0.83 (0.07) | 2.08×10^{-9} (0.01) |
| Ratio 1:4% | 2.56 | 1.42 | 1.36 | 1.40 | 0.6 | 1.00 |

^aMean values among three experiments.

^bMeans of standard deviations for the regions imaged.

the data in such a way to demonstrate the degree of inhomogeneity which characterises calcium alginate gels. Standard deviations for the region imaged, selected for each gel in such a way to leave the middle band out, are reasonably small; this demonstrates that the gels are quite homogeneous if we do not consider the band in the middle which presents a much lower alginate concentration.

The data presented in Table 2 demonstrate that of all the water MRI parameters measured, the T_2 relaxation time and K were the most sensitive to alginate concentration (by 2.6- and 0.6-fold, respectively) and therefore the most suitable for determining gel strength. A linear relationship between $1/T_2$ and gel concentration had already been found for alginate systems [11], so this work confirms the usefulness of quantitative MRI to map polymer content non-invasively.

The longitudinal relaxation time (T_1) proved to be less sensitive than T_2 to gel concentration: the T_1 value decreased by about 30% from 1% (w/w) to 4% (w/w) gel concentration, in comparison with a decrease of more than 60% for T_2 . The same overall mechanism is responsible for both T_1 and T_2 relaxation, but an additional dependence on very slow molecular motion further enhances the sensitivity of T_2 -values to restricted mobility.

The water self-diffusion coefficient (D) was the same for all the alginate gel concentrations; indeed the values were only marginally smaller than the value ($2.25 \times 10^{-9} \text{ m}^2/\text{s}$) for a water phantom at the same temperature (T 24 °C). This demonstrates that the alginate gel matrix does not significantly hinder the diffusive motion of water molecules, which are free to diffuse inside the gel; this is in accordance with previous data which indicate [5] that diffusion of small molecules is very little affected by an alginate matrix.

Magnetisation transfer processes are known to be quite efficient in alginate gels for which they are strongly influenced by gel concentration [14]; the amount of polymer affects the proportion of exchangeable sites ($-\text{OH}$), which are the crucial factor for the observed phenomenon. From the MT experiments, values of M_{sat} , M_0 and $T_{1\text{sat}}$ were determined by fitting the data according to Eq. (3) (Section 4) and the proton exchange rate (K) was then calculated from Eq. (4). The variation in K with gel concentration was significantly larger than the variation in either the $T_{1\text{sat}}$ or M_{sat}/M_0 ratio, because of the combined effect of the decrease in both $T_{1\text{sat}}$ and M_{sat}/M_0 ratio, observed at higher concentrations.

In what follows, we shall discuss the two most useful parameters (T_2 and K) and their mechanisms; since both those relaxation processes depend on molecular motion to generate randomly varying magnetic fields, we can infer valuable information about those motions, especially from T_2 . The mechanism responsible for spin–spin relaxation involves magnetic interactions between the protons on different molecules, which induce an exchange of energy between those protons. In a rigid structure, or one in which the relative motion between the protons is slow, the process is quite efficient and T_2 -values are short. Alginate molecules in solution, and even more so in gels, induce an increase in the structure of the surrounding water: thus, the ‘bound’ water molecules which are chemisorbed to the surface of the polysaccharide molecules have a lower degree of mobility than those of bulk water. Consequently, when chemical exchange occurs between them and the hydroxyl protons of the alginate molecule, the measured T_2 relaxation time is a weighted mean of all the different environments which the water molecules have experienced during that measurement (‘bound’ and ‘free’ pools); chemical exchange between water protons and hydroxyl protons of alginate molecules is thought to be the main mechanism responsible for proton relaxation in gels [15].

The MT experiment involves the saturation of the broad proton resonance of the macromolecules using a frequency-selective radio frequency pulse, without directly affecting the narrow resonance of the protons of the mobile water pool. The resultant decrease in the magnetisation of the bulk water is the result of an exchange between the saturated protons on the macromolecules and the unsaturated protons of the aqueous medium. Two different mechanisms are responsible for this exchange: cross-relaxation, which is enhanced at the water–molecule interface, and chemical exchange with the hydroxyl and carboxyl groups on the surface of a relatively immobile polymer matrix. Even though sodium alginate contains the same number of exchangeable protons no significant MT effect was observed because the motion of the alginate molecules is too fast.

Prompted by the above, four alginate samples with different *O*-acetyl contents were studied to evaluate the use of MRI to discriminate between them; these acetylated samples were the same as those used by Skjåk-Bræk et al. [9] for their work. The gel from the non-acetylated sample (0% OAc) was prepared at a concentration of 2% (w/w), and the weight of the other samples was corrected accordingly in order to

obtain the same concentration of uronate residues. The results presented in Table 3 illustrate how the various water NMR parameters are influenced by the different *O*-acetyl content of the four samples. It is important to note that no comparison can be made with the values presented in Table 2 for the commercial sample, because of the difference between the samples in the amount of guluronic acid, in the molecular weight, and in the purification procedures used.

As expected, both T_2 and K were very sensitive to gel strength, which seemed to be seriously compromised for samples with high degree of acetylation (d.a.). Thus, for both the T_2 and K values, there was a roughly two-fold difference between the values for low d.a. (T_2 , 75–102 ms; K , 0.47–0.55 L/s) compared to those for the two samples with higher d.a. (T_2 , 222–190 ms; K , 0.23–0.27 L/s). There was a dramatic decrease in gel strength as the amount of acetyl groups increased from 10.3 to 47.6%, whereas it remained practically constant for the samples with d.a. equal to 117%. This proves once again [9] that *O*-acetylation on both guluronic and mannuronic residues inhibits the formation of strong gels which have good mechanical properties: when the content of *O*-acetyl groups is high, the mechanism responsible for gel formation, which involves the hydroxyl groups on unsubstituted guluronate acid residues, fails to induce a high degree of conformational ordering of the chains.

The sample with 10.3% d.a. presented a shorter T_2 than the non-acetylated sample; this finding seems not to be in accord with the results presented by Skjåk-Bræk et al. [9], who showed a decrease of the modulus of rigidity, even at low values of acetylation. The decrease in T_2 for the sample with 10.3% d.a. can be explained if we consider the fact that a small amount of acetylation, mostly present on the chain regions not directly involved in the gelation with calcium, plays an important role in the water ordering and in the total amount of 'bound' water,

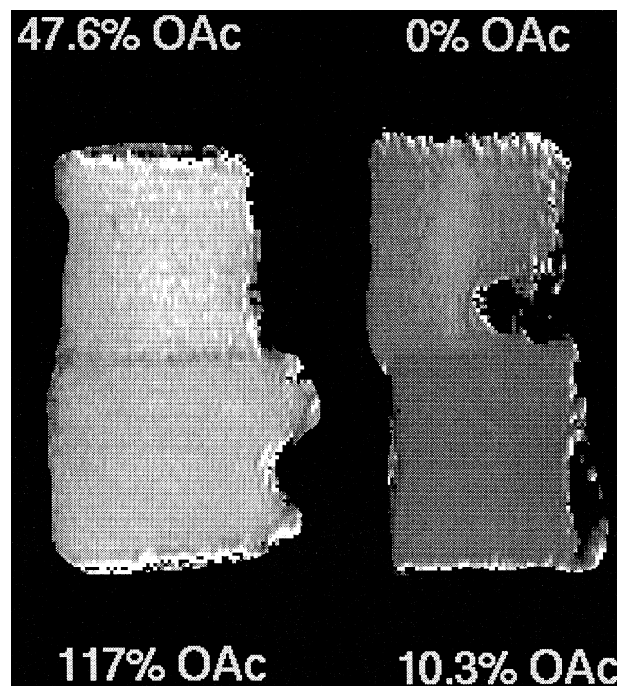


Fig. 2. T_2 -map for alginate gels with different *O*-acetyl content: gels with a high d.a. (47.6 and 117%) have a higher value of T_2 which implies a markedly reduced gel strength when compared with the non-acetylated or low *O*-acetyl content gels (0 and 10.3%). The *O*-acetylated samples have been prepared from *Laminaria hyperborea* and the gels were obtained dialysing Na-alginate solutions against 0.06 M CaCl_2 containing 0.2 M NaCl.

chemisorbed to those regions. In support of this, Skjåk-Bræk et al. found an increased degree of swelling for the acetylated samples; the higher gel homogeneity we obtained for the acetylated samples (Fig. 2) can be explained in terms of a slower swelling kinetics [9], which favours the approach to equilibrium. While for higher degrees of acetylation the mechanical properties, such as the modulus of rigidity, better explain the observed increase in T_2 , for samples with low values of acetylation, the swelling phenomenon becomes predominant, leading to a shortening of the T_2 values.

Table 3

NMR parameters: MRI measurements for alginate gels with different acetyl content (% OAc); alginate gels have been obtained dialysing alginate solutions against 0.06 M CaCl_2 containing 0.2 M NaCl

| % OAc | T_2 (ms) | T_1 (s) | $T_{1\text{sat}}$ (s) | M_{sat}/M_0 | K (L/s) |
|--------------|------------------------|-------------|-----------------------|----------------------|-------------|
| 0% | 102 (7.5) ^a | 2.42 (0.09) | 1.31 (0.08) | 0.39 (0.01) | 0.47 (0.04) |
| 10.3% | 75 (3.5) | 2.47 (0.08) | 1.15 (0.09) | 0.35 (0.02) | 0.55 (0.06) |
| 47.6% | 222 (5) | 2.44 (0.08) | 1.84 (0.16) | 0.58 (0.02) | 0.23 (0.02) |
| 117% | 190 (14) | 2.72 (0.07) | 1.78 (0.15) | 0.52 (0.01) | 0.27 (0.02) |
| Ratio 117:0% | 1.86 | 1.12 | 1.36 | 1.33 | 0.57 |

^aThe values in brackets represent the standard deviation for the region imaged.

3. Conclusion

In this work, we have used a fully automated MRI analysis protocol to measure the MRI parameters of water in alginate solutions and gels, and have established that those parameters provide spatial characterisation of the chemistry of the alginate matrices considered. The T_2 relaxation time and the proton exchange rates appear to give very useful information about molecular motion, and provide good insight to how differences in chemical structure can influence functional properties, such as mechanical strength and diffusion properties, at least in alginate gels.

4. Experimental

Samples.—The commercial sample of alginate containing 35% of guluronic acid was obtained from FISONS Scientific Apparatus. The *O*-acetylated samples, containing 68% of guluronic acid (acetyl content, 0%, 10.3%, 47.6%, 117%), were prepared from *L. hyperborea* [15]. Sodium alginate solutions at different concentrations (% w/w) were prepared by dissolving the samples in 0.2 M NaCl. Calcium alginate gels were made by pouring the alginate solution into a plastic cylinder (i.d. 1.2 cm; height 1.3 cm) fitted with a dialysis membrane at each end, and dialysing for 72 h against 0.06 M CaCl_2 containing 0.2 M NaCl; the sodium ions were added to increase the homogeneity of the gels [13].

MRI instrumentation.—All the measurements were performed on a Bruker Medizin Technik Biospec II console, coupled to an Oxford Instruments 31 cm horizontal bore superconducting magnet operating at 2.35 T (100 MHz for ^1H). All the samples were studied using a 2.4 cm diameter birdcage radio frequency coil inside a 11.6-cm diameter gradient set that provided maximum magnetic field gradients of 0.16 T/m.

Imaging protocols.—All the images were acquired with a 256×128 pixel matrix, 5 cm Field of View, 3 mm slice thickness, $195 \mu\text{m}/\text{pixel}$ in plane resolution and 2 averages. Quantitative MRI maps of T_1 , T_2 , $T_{1\text{sat}}$, M_{sat}/M_0 ratio, and MT rates (K) were achieved by varying successively the recovery delay (RD), the echo time (T_E), and the saturation transfer delay (SP) in a multi-echo (CPMG) MRI sequence. The saturation pulse was a squared pulse of low amplitude (0.1 G) and 10 kHz off-resonance, applied before NMR excitation.

For T_2 maps, 12 images were acquired with an

inter echo time of 20 ms; data from the same pixel in each of these images were fitted to a single exponential decay, according to the equation:

$$M = M_0 \exp(-T_E/T_2) \quad (1)$$

where M_0 represents the proton density and hence the relative distribution of water protons within the sample.

Variable delay lists for T_1 and $T_{1\text{sat}}$ weighted images were based on a logarithmic scale with 7 and 8 points, respectively, with RD and SP incremented to values of 12.5 and 6 s, respectively. Maps of T_1 , $T_{1\text{sat}}$, M_{sat}/M_0 were obtained by fitting the data to equations:

$$M = M_0 [1 - \exp(-RD/T_1)] \quad (2)$$

$$M = M_{\text{sat}} + (M_0 - M_{\text{sat}}) \exp(-SP/T_{1\text{sat}}) \quad (3)$$

where M_0 is the equilibrium longitudinal magnetisation in the absence of saturation transfer, M_{sat} is the minimum longitudinal magnetisation when saturation transfer has reached a steady state ($SP \cong 5 \times T_{1\text{sat}}$), and $T_{1\text{sat}}$ is the longitudinal relaxation time measured during saturation exchange between macromolecular and water protons. The proton exchange rate (K) was then given by:

$$K = 1/T_{1\text{sat}} (1 - M_{\text{sat}}/M_0) \quad (4)$$

Water self-diffusion coefficients (D) experiments were performed by varying the gradient pulse amplitude in a Pulsed Field Gradient (PFG) NMR sequence. Data were analysed by nonlinear least-squares regression of the equation:

$$M/M_0 = \exp[-(\gamma g \delta)^2 (\Delta - \delta/3) D] \quad (5)$$

where γ is the proton magnetogyric ratio, g is the pulsed field gradient intensity, δ is the duration of the field gradient pulse, and Δ is the time interval between the leading edges of the field gradient pulses.

Bulk NMR measurements.—Bulk T_1 measurements were made using an inversion-recovery sequence, in which the inversion time was incremented from 0 to 15 s, according to a logarithmic scale of 32 points. Similarly, $T_{1\text{sat}}$, M_{sat}/M_0 and K were measured using an inversion saturation recovery sequence, with a saturation delay varied from 0 to 4 s, according to a logarithmic scale of 12 points. A CPMG sequence was used to measure T_2 , with an inter echo time of 8 ms.

Computing.—All data were processed on a Sun Sparc station model, running UNIX, C-code software developed in house. All the values were obtained,

either from imaging or ‘bulk’ measurements, by fitting the data with a curve fitting program, based on the Levenburg–Marquardt nonlinear least-squared minimisation algorithm [16].

Acknowledgements

It is a pleasure to thank the University of Trieste for a scholarship (A.D.), and the Herchel Smith Endowment for financial support of this work. We also thank Drs. P.J. Watson and J.J. Tessier for the development of the automated MRI protocol used in this study.

References

- [1] A. Johansen and J.M. Flink, *Enzyme Microb. Technol.*, 8 (1986) 145–148.
- [2] O. Smidsrød and G. Skjåk-Bræk, *TIBTECH*, 8 (1990) 71–78.
- [3] G. Skjåk-Bræk, *Biochem. Soc. Trans.*, 20 (1992) 27–33.
- [4] P. Lundberg, S.J. Berners-Prico, R. Sushmuta, and P.W. Kuchel, *Magn. Reson. Med.*, 25 (1992) 273–288.
- [5] G.T. Grant, E.R. Morris, D.A. Rees, P.J.C. Smith, and D. Thom, *FEBS Lett.*, 32 (1973) 195–198.
- [6] A. Martinsen, G. Skjåk-Bræk, and O. Smidsrød, *Biotechnol. Bioeng.*, 33 (1989) 79–89.
- [7] A. Martinsen, I. Storrø, and G. Skjåk-Bræk, *Biotechnol. Bioeng.*, 39 (1992) 186–194.
- [8] H. Tanaka, M. Matsumura, and I.A. Veliky, *Biotechnol. Bioeng.*, 26 (1984) 53–58.
- [9] G. Skjåk-Bræk, F. Zanetti, and S. Paoletti, *Carbohydr. Res.*, 185 (1989) 131–138.
- [10] K.I. Draget, K. Ostgaard, and O. Smidsrød, *Carbohydr. Polym.*, 14 (1991) 159–178.
- [11] K. Potter, T.A. Carpenter, and L.D. Hall, *Carbohydr. Res.*, 246 (1993) 43–49.
- [12] K. Potter, B.J. Balcom, T.A. Carpenter, and L.D. Hall, *Carbohydr. Res.*, 257 (1994) 117–126.
- [13] G. Skjåk-Bræk, H. Grasdalen, and O. Smidsrød, *Carbohydr. Polym.*, 10 (1989) 31–54.
- [14] J.J. Tessier, K. Potter, T.A. Carpenter, and L.D. Hall, *Magn. Reson. Chem.*, 32 (1994) 55–61.
- [15] B.P. Hills, K.M. Wright, and P.S. Betton, *Mol. Phys.*, 67 (1989) 1309–1326.
- [16] W.H. Press, S.A. Flannery, S.A. Tenkolsky, and W.T. Vetterling, *Numerical Recipes in C: The Art of Scientific Computing*, Chap. 8, Cambridge Univ. Press, New York, 1988.